7311-EN-09
DTIC

Prediction of Mouth Bar Development and Deformation for Navigation Purposes

Final Technical Report

by
Alexander N. Butakov

January 1996

United States Army
European Research Office of the U.S. Army
London England

Contract Number N68171-95-C-9032, Alexander N. Butakov

Approved for Public Release; distribution unlimited

19960212 191

DTIC QUALITY INSPECTED 4

REPORT DOCUMENTATION PAGE			
1.	2. 29 January 1996	3. final report, 03/01/95-11/30/95	
4. Prediction of Mouth Bar Development and Deformation for Navigation Purposes.			5. Contract N68171-95-C-9032
6. Professor Alexander N. Butakov			
7. Friendship University of Russia Engineering Department 6 Miklukho-Maklaya Street Moscow, 117 198 GSP Russia			8. Report N3
9. USARDSG-UK Environmental Sciences Branch Edison House 223 Old Marylebone Road London NW1 5TH United Kingdom			10.
11. The Research reported in this document has been made possible through the support and sponsorship of the U.S. Government through its European Research Office of the U.S. Army. This report is intended only for the internal management use of the Contractor and U.S. Government.			
12a.			12b

13. **Abstract**

A new theoretical model for the development of an estuary bed profile under the influence of river flow is presented. The model is based on original dependences describing the distribution of the free-water surface slope both along and across the mouth reach that were developed by an analysis of experimental data. A fundamentally new solution is given, which accounts for the turbulent interactions between flow jets in the coastal area where the river flow actively interacts with the surrounding water.

Two variants of the theoretical model were formulated, a one-dimensional and a two-dimensional model (a flow plan). Numerical solution of the one-dimensional model allowed prediction of bottom deformations with time under the influence of key hydrological factors at different slopes of coastal bottom relief. Numerical solution of the flow plan model provided the longitudinal and transverse distributions of flow velocities and bottom relief deformations.

An analysis of the obtained information afforded novel dependences describing the rates of bottom relief formation and bar crest growth, as well as the final height of the bar crest and the rate of its downstream migration. The results of calculations are in perfect agreement with the experimental data and field measurements. The results of this work will help choosing the right location and depth of navigable channels in estuaries.

14. Mouth bar, Estuary, Navigation draft, Numerical simulation			15. 19 Pages
			16.
17. Unclassified	18 Unclassified	19. Unclassified	20.

Table of Contents

Technical Objective

The objective of this work was to create a universal theoretical description of the development and deformations of mouth bars caused by a combination of river and sea hydrological factors. The developed model assumes the absence of considerable tidal and sea-wave influence on the mouth bar relief. Development of such a theory should be considered as a substantial contribution to hydrology.

The proposed numerical model allows prediction of 1) mouth bar deformations due to seasonal changes in the hydrological regimes of both river and sea and 2) obstruction of the navigable channel under the influence of active factors in various combinations. Successful solution of this problem opens new horizons in the prediction of mouth bar deformations.

Background

The cyclic development of delta branching is extensively studied by drilling and documented in archive sources [1]. The redistribution of flow in delta branches has an adequate theoretical description [2,3]. Unlike these processes, the morphological changes in bar relief that occur under the combined influence of river and sea hydrological factors have no analytical solution as yet. Only a few rough approximations such as the so-called "mouth elongation" can be found in the literature [4]. Our extensive experimental studies [5,6,7], examination of actual data on numerous river estuaries (in particular, those of rivers flowing into the marginal seas of the Arctic Ocean [7,8]), and theoretical calculations [9,10,11] constituted the elements of a universal theory of mouth bar development [7,12,13]. Fragmentary realisations of this theoretical model were successful [14,15,16].

The theory of the problem

Navigational traffic in river estuaries requires practical knowledge about the intensity of sedimentation in the estuary, mouth bar development, navigational depth at the bar crest, and the rate of migration of bar elements. In the case being considered, the navigation-affecting parameters of a mouth bar totally depend on river factors. The mouth bar development mainly occurs at high-water periods (floods), when the bar crest reaches its maximum height and the bar itself is maximum shifted seawards. This time is least favourable for navigation. Sea factors, especially wind-induced waves, usually destroy the bar relief formed by river flow, restructure it, and lower the bar crest. Such deformations often increase navigational depths. However, the effect of sea factors on the stability and profile of a navigable channel is ambiguous. The river- and sea-related processes, which are often counteracting, will be discussed elsewhere.

Variations of the bar crest height with time, the rate of its vertical deformation and longitudinal migration, as well as other parameters that depend on annual and perennial changes in river runoff, free-water surface slope, and sediment discharge at the upper boundary of the estuary reach will subsequently be referred to as the "mouth bar regime".

The estuary area is usually subdivided in two regions [4]: the estuary reach where river factors dominate and the coastal area with distinctly sea-type hydrological regime. The upper boundary of the estuary reach normally coincides with either the delta head or the section line at which no positive set-up can be observed. The lower boundary is a virtual line enveloping either the sea coast or delta islets reached by the sea. Section line at which the influence of the river flow disappears separates the coastal area from the open sea.

The theoretical model uses the system of orthogonal curvilinear co-ordinates shown in Fig. 1. The origin of co-ordinates is in the centre of the estuary section line. The longitudinal co-ordinate l is directed downstream. The upper and lower boundaries of the estuary area (as defined above) were assumed to be at $-\infty$ and $+\infty$, respectively. In the one-dimensional model, flow velocities and bottom deformations are either considered along the stream axis (the isoline of maximum depths) or averaged across the flow. In the two-dimensional model, the river flow is divided into separate flow jets. This approach known as the construction of a flow plan simplifies both the set-up and solution of the

problem compared to the use of orthogonal co-ordinates. The ordinate axis is denoted b axis. Flow velocities are averaged over depth.

The behaviour of the free-water surface slope

It is known that the free-water surface slope of a river depends on such parameters as bed profile, bed roughness, and flow rate and is mainly determined by the surface drop between the upper boundary of the estuary reach and the reservoir level. As water level at the upper boundary greatly varies, whereas the sea level is constant, the maximum surface slope should correspond to catastrophic floods, and the minimum slope, to low-water periods.

River flow above the estuary is usually considered to be quasi-uniform, with a constant surface slope along the river bed. Within the estuary reach, river flow is always non-uniform. Here the surface slope is increasing downstream at high-water periods and reaches its maximum at the estuary section line (Fig. 1). Location of the maximum slope depends on flood intensity. The higher the flood, the more the section line of maximum surface slope is shifted seawards. Within the coastal area, the surface slope is first sharply decreased (as the river flow is no longer confined between the banks) and then gradually disappears. At low-water periods, a continuous decrease of the surface slope down the river is observed virtually everywhere along the estuary reach. Within the coastal area, the surface slope is only observable at the bar crest during negative wind-induced set-ups.

A statistical analysis of experimental results and field measurements provided an analytical expression of the surface slope behaviour. The slope depends on 1) the surface slope above the estuary area $I_{-\infty}$, 2) the positive difference ΔZ_{W_0} between the surface level at the estuary section line that would be observed in the case of quasi-uniform water flow within the estuary reach and the reservoir level (Fig. 1), and 3) the morphological index k_T of the river bed:

$$I = I_{-\infty} + I_{-\infty} a_I e^{k_T C_k' \tilde{l}} \quad \text{at } \tilde{l} \le 0, \tag{1}$$

$$I = I_0 e^{-k_T C_k'' \tilde{l}} \quad \text{at } \tilde{l} > 0, \tag{2}$$

where $I_0 = (1 + a_I) I_{-\infty}$ is the surface slope at the estuary section line,

a_I is the slope amplitude,

C_k' and C_k'' are the parameters of the estuary reach and coastal area, respectively, that determine the degree of the surface slope transformation;

$k_T = \lambda_T B_{-\infty} / H_{-\infty}$ is the morphological parameter of the river bed

where λ_T is the hydraulic friction coefficient,

$B_{-\infty}$ and $H_{-\infty}$ are the average width and depth of the bed, respectively, above the estuary area,

$\tilde{l} = l / B_{-\infty}$ is the relative distance from the estuary section line.

An expression for the longitudinal profile of the free-water surface is found by direct integration of (1) and (2):

$$Z_W = Z_{W_{-\infty}} - I_{-\infty} B_{-\infty} \tilde{l} - I_{-\infty} B_{-\infty} \frac{a_I}{k_T C_k'} e^{k_T C_k' \tilde{l}} \quad \text{at } \tilde{l} \le 0,$$

$$Z_W = I_{-\infty} B_{-\infty} \frac{(1 + a_I)}{k_T C_k''} e^{-k_T C_k'' \tilde{l}} \quad \text{at } \tilde{l} > 0 \tag{3}$$

where $\bar{Z}_W$ and $\bar{Z}_{W_{-\infty}}$ are the free-water levels (measured with respect to the constant level of calm sea) in the river bed and at the upper boundary of the estuary reach (the initial section), respectively.

The slope amplitude a_I can be determined using the limiting condition of smoothness (the absence of discontinuities) imposed on the curve that represents the free-water surface at the estuary section line:

$$\left.\frac{dZ_W}{dl}\right|_{l\to-0} = \left.\frac{dZ_W}{dl}\right|_{l\to+0} \quad \text{or} \quad I|_{l\to-0} = I|_{l\to+0}.$$

This condition together with (1) and (2) gives the following expression for the slope amplitude:

$$a_I = \left(\frac{\Delta Z_{W_0} k_T}{I_{-\infty} B_{-\infty}} - \frac{1}{C_k''}\right)\frac{C_k' C_k''}{C_k' + C_k''}, \tag{4}$$

whence ΔZ_{W_0}, which is the sum of free-water level drops within the estuary reach and coastal area (Fig. 1), is determined:

$$\Delta Z_{W_0} = \left(\frac{a_I}{C_k'} + \frac{1+a_I}{C_k''}\right)\frac{I_{-\infty} B_{-\infty}}{k_T}.$$

No theoretical justification of the C_k' and C_k'' values exists as yet. In the present model, these parameters are free variables determined by comparing the experimental data with the results of numerical modelling. Either parameter may be greater or less than unity. An analysis of experimental data and field measurements showed that the curve representing the free-water surface is smoothed during the development of a mouth scour and formation of the bar crest with both the discharge and level of water in the initial section being constant. This smoothing can be accounted for by decreasing the C_k parameters. A simple empirical formula was discovered:

$$C_k' = C_k'' = C_k = 1/\tilde{H}_{\max},$$

where $\tilde{H}_{\max} = H_{\max}/H_{-\infty}$,

$H_{\max}$ is the maximum depth of mouth scour, and

$H_{-\infty}$ is the river depth above the initial section.

Assuming that $C_k' = C_k'' = 1$ at $t = 0$, formula (4) can be transformed to express the slope amplitude as a function of time:

$$a_I(t) = 0.5\left[\left(1 + 0.5 a_I(0)\right)C_k - 1\right].$$

It should be noted that the slope amplitude a_I and parameters C_k' and C_k'' may differ for each of the jets in the flow plan model. In general, they are gradually decreasing upon transition towards peripheral jets.

Flow velocity within the estuary reach

Water flow within the estuary reach is both non-uniform and unsteady. However, the performed tests and comparisons (e.g., see [17]) show that the term accounting for the local acceleration in the differential equation of motion is negligible compared to other terms even during build-ups and recessions of natural floods. It was shown that the turbulent tangential stress can also be neglected in this case [10]. Therefore, the initial equation can be written as follows:

$$I = \frac{d}{dl}\left(\frac{V^2}{2g}\right) + \frac{\lambda_T}{H}\frac{V^2}{2g} \text{ at } \tilde{l} \le 0. \quad (5)$$

Here, V and H are the flow velocity and depth for a given cross-section. The solution of (5) can be written in this form [5]:

$$V^2 = 2g \int_{-\infty}^{l} Ie^{-\int_x^l \lambda_T \frac{dx}{H}} dx. \quad (6)$$

For an open bed, the hydraulic friction coefficient λ_T can be expressed via the Chézy friction factor C as $\lambda_T = 2g / C^2$. Using the Manning formula for the Chézy factor and assuming a constant coefficient of bed roughness along the flow, we obtain the following equation, in which the hydraulic friction coefficient is expressed via its value in the initial section (viz., at the upper boundary of the estuary reach):

$$\int_{-\infty}^{l} \frac{\lambda_T}{H} dl = \lambda_{T_{-\infty}} H_{-\infty}^{m_1 - 1} \int_{-\infty}^{l} \frac{dl}{H^{m_1}} = \lambda_{T_{-\infty}} F(l),$$

where $\lambda_{T_{-\infty}}$ is the hydraulic friction coefficient for the initial section and $m_1 = 4/3$.

Substitution of this expression and that of the surface slope (1) in (6) followed by reduction to a non-dimensional form gives

$$U = A' k_T \left[\int_{-\infty}^{\tilde{l}} e^{-k_T \theta(\tilde{l}, \tilde{x})} d\tilde{x} + a_I \int_{-\infty}^{\tilde{l}} e^{k_T \left[-\theta(\tilde{l}, \tilde{x}) + C_k' \tilde{x} \right]} d\tilde{x} \right] \quad (7)$$

where $U = \frac{V^2}{V_{-\infty}^2}$, $\theta(\tilde{l}, \tilde{x}) = \int_{\tilde{x}}^{\tilde{l}} \frac{d\tilde{l}}{\tilde{H}^{m_1}}$, $\tilde{l} = \frac{l}{B_{-\infty}}$, and $\tilde{H} = \frac{H}{H_{-\infty}}$.

As water flow in the initial section is assumed to be quasi-uniform,

$$A' = \frac{2gI_{-\infty}B_{-\infty}}{V_{-\infty}^2 k_T} = 1$$

The obtained expression (7) is valid both in the one-dimensional and two-dimensional (flow plan) models.

Let us consider the initial stage of bottom relief formation, when the depth is constant along the river bed. In this case, (7) takes this simple form:

$$U = 1 + \frac{a_I}{1 + C_k'} e^{k_T C_k' \tilde{l}} \quad (8)$$

Flow velocity within the coastal area

Within the coastal area, the river flow spreads unconfined by the banks, which results in active turbulent interactions between the river flow and the surrounding water mass. This process, as well as bottom friction, efficiently quenches the flow energy and decreases its velocity. In this case,

equation (5) should be complemented with a term accounting for the tangential stress on the lateral surfaces of flow jets [10].

Methods of calculating breakdown flows applicable to river flows as well were developed by numerous researchers [18,19,20,21,22]. Vast experimental data on the expansion of breakdown flows can be found in [19,23]. A solution of the problem accounting for the bottom friction and turbulent tangential stress in the case of both free-water surface slope and depth varying along the river was reported in our earlier works [9,10,24].

Given a preferred flow direction, so that the velocity vector is practically collinear with the longitudinal co-ordinate, the simplest expression for the turbulent tangential stress is

$$\tau = \rho \nu_t \frac{\partial V}{\partial b},$$

where the turbulent viscosity coefficient ν_t is a scalar.

The up-to-date models of turbulence, e.g. the differential $K - \varepsilon$ model, seem to be the best founded from the theoretical viewpoint. However, application of such models to the discussed problem would have considerably complicated the analytical expressions for stream velocities with only a small gain in accuracy. Therefore, we favoured the hypothesis of V.M. Makkaveev [25] that the turbulent viscosity coefficient is proportional to averaged velocity, viz.

$$\nu_t = \Lambda V,$$

where Λ is a function with linear dimensionality.

To deduce an equation for the velocity distribution in a free turbulent jet, I.M. Konovalov [26,27] treated the diameter (width) of the expanding jet as a characteristic dimension and expressed it as a linear function of the longitudinal co-ordinate. The resulting expression for ν_t was

$$\nu_t = 2a^2 lV \tag{9}$$

where a is the turbulent exchange coefficient.

A similar dependence was earlier discovered by Reichardt [28] who analysed the experimental data on the velocity distribution in a turbulent jet. The phenomenological theory of Reichardt attracted serious criticism. Nevertheless, it is in a good agreement with the experimental data and has undeniable practical advantages [29]. Assuming the Reichardt--Konovalov definition of the turbulent viscosity coefficient, we arrive at the following differential equation of flow motion that includes all the key factors of turbulence:

$$2a^2 l \frac{\partial^2}{\partial b^2}\left(\frac{V^2}{2g}\right) \equiv \frac{\partial}{\partial l}\left(\frac{V^2}{2g}\right) + \frac{\lambda_T}{H}\frac{V^2}{2g} - I \text{ at } l > 0.$$

Substituting $V^2 = ue^{-\lambda_T F(l)}$, $I = -\frac{\partial z}{\partial l}e^{-\lambda_T F(l)}$, and $\Phi = u/2g + z$, one obtains

$$a^2 \frac{\partial^2 \Phi}{\partial b^2} = \frac{\partial \Phi}{\partial\left(l^2\right)} \tag{10}$$

As river flow practically expands in the coastal area as in an unbounded half-space, the initial conditions are

$$\Phi|_{l=0} = \Phi(\alpha) = V_0^2/2g + z_0, \text{ if } -B_0/2 \le b \le B_0/2,$$

$$\Phi|_{l=0} = 0, \text{ if } \begin{cases} b > B_0/2 \\ b < -B_0/2 \end{cases},$$

where V_0 and z_0 are the flow velocity and the z value, respectively, in the mouth section.

Following is the solution of (10):

$$\Phi = \frac{1}{2al\sqrt{\pi}} \int_{-B_0/2}^{B_0/2} \Phi(\alpha) e^{-\left(\frac{\alpha-b}{2al}\right)^2} d\alpha.$$

Flow velocity can be written as

$$V^2 = \left[V_0^2 \Sigma\Psi + 2gz_0(\Sigma\Psi - 1) + 2g\int_0^l Ie^{\lambda_{T_0} F(l)} dl \right] e^{-\lambda_{T_0} F(l)}, \quad (11)$$

where $\Sigma\Psi = \frac{1}{2}\left[erf\left(\frac{1/2 + b/B_0}{2al/B_0} \right) + erf\left(\frac{1/2 - b/B_0}{2al/B_0} \right) \right]$,

$erf(x) = \frac{2}{\sqrt{\pi}} \int_0^x e^{-t^2} dt$ is the error function,

$$F(l) = H_0^{m_1 - 1} \int_0^l \frac{dl}{H^{m_1}},$$

B_0 and H_0 are the bed width and depth, respectively, in the mouth section,

λ_{T_0} is the hydraulic friction coefficient in the mouth section.

Changing over to dimensionless values and taking account of the expression (2) for the surface slope, one can write

$$U = \left[U_0 \Sigma\Psi + (U_{00} - U_0)(\Sigma\Psi - 1) \right] e^{-k_T \theta(\tilde{l}, 0)} + \\ + (1 + a_I) k_T \int_0^{\tilde{l}} e^{-k_T \left[\theta(\tilde{l}, \tilde{x}) + C_k'' \tilde{x} \right]} d\tilde{x}, \quad (12)$$

where $U_0 = \frac{V_0^2}{V_{-\infty,0}^2}$, $U_{00} = \frac{V_{00}^2}{V_{-\infty,0}^2}$,

V_{00} and $V_{-\infty,0}$ are the axial flow velocities in the mouth section and at the upper boundary of the estuary reach, respectively.

The solution (12) is valid at any point along the river flow where the confining banks do not substantially affect the flow motion. In the particular case of the one-dimensional model, flow velocity is described by the following expression:

$$U = U_0 \Sigma\Psi e^{-k_T \theta(\tilde{l},0)} + (1+a_I) k_T \int_0^{\tilde{l}} e^{k_T\left[-\theta(\tilde{l},\tilde{x}) - C_k'' \tilde{x}\right]} d\tilde{x}, \quad (13)$$

where $\Sigma\Psi = erf\left(\frac{B_0}{4al}\right)$.

At the initial stage of bottom relief formation, the depth is everywhere constant, therefore

$$U = \left[U_0 \Sigma\Psi + \frac{1+a_I}{1-C_k''}\left(e^{k_T(1-C_k'')\tilde{l}} - 1\right)\right] e^{-k_T \tilde{l}} \quad (14)$$

There is an alternative non-dimensional representation of (11) for the case of an axial jet:

$$\frac{V^2}{V_0^2} = \Sigma\Psi e^{-k_T \theta(\tilde{l},0)} + A'' k_T \int_0^{\tilde{l}} e^{k_T\left[-\theta(\tilde{l},\tilde{x}) - C_k'' \tilde{x}\right]} d\tilde{x},$$

where $A'' = \frac{2gI_0 B_{-\infty}}{V_0^2 k_T}$.

Let us consider the physical meaning of parameter A''. As was shown above, $A' = 1$ in the initial section regardless of water level. In the mouth section, A'' can be either greater or less than unity, i.e. $A'' > 1$ during floods and $A'' < 1$ during low-water periods. It follows from (3) that the positive difference between the free-water surface level in the mouth section and the stable sea level is

$$\Delta Z_{W_2} = \frac{I_0 B_{-\infty}}{k_T C_k''} = \frac{(1+a_I) I_{-\infty} B_{-\infty}}{k_T C_k''}.$$

Substitution of this formula in the above expression for A'' gives:

$$A'' = \frac{\Delta Z_{W_2}}{\left(V_0^2 / 2g\right)} C_k'',$$

This is a ratio between the excess specific potential energy of the flow in the mouth section with respect to the reservoir level and the specific kinetic energy of the flow in the same section multiplied by C_k''.

Assuming $C_k'' = 1$, one arrives at a simple relationship between the distribution of velocities along the coastal area and the quotient $\Delta Z_{W_2} / \left(V_0^2 / 2g\right)$. Thus, when the potential energy of the flow jet is greater than its kinetic energy, there occurs a partial transition of the former into the latter. Accordingly, the flow is accelerated, and its velocity reaches a maximum at some distance downstream from the mouth section. Then, the flow velocity gradually decreases due to turbulent and frictional dissipation of energy. If the potential and kinetic energies are equal, the flow velocity slowly decreases along the longitudinal co-ordinate, so that $\left.\frac{dV}{dl}\right|_{l=0} = 0$. If the potential energy is less than the kinetic energy, the flow jet velocity abruptly falls as soon as the flow reaches the coastal area.

Bottom relief deformations

Bottom deformations of the estuary reach and mouth bar depend on the actual discharge of bed load, which is determined by the hydraulic characteristics of the flow in any cross-section of the river bed. Our investigations showed the distribution of sediments along the river to be a function of flow velocity. The streamwise migration of sediments is practically unaffected by depth changes. This together with the fact that the water discharge is constant along the flow trajectory gives an expression for the rate of vertical deformations of the river bed and mouth bar:

$$\varsigma = -\frac{dH}{dt} = \frac{q_{s\_\infty}}{(1-\varepsilon)B_{\_\infty}} U\left(\frac{U}{\tilde{H}}\frac{\partial \tilde{H}}{\partial \tilde{l}} - \frac{3}{2}\frac{\partial U}{\partial \tilde{l}}\right), \tag{15}$$

where q_{s_∞} is the sediment discharge in the initial section (volume units per unit of bed width) and

ε is the porosity coefficient of bottom sediments.

The maximum amount of bed load that can be displaced by river flow under given hydrological conditions is determined using the following original formula:

$$q_s = 0.0065\left(\frac{\nu}{\sqrt{g}}\right)^{1/3}\sqrt{d}V_n\left(\frac{V}{V_n}\right)^4, \tag{16}$$

where V_n is the non-displacing velocity defined by V.N. Goncharov [30] as $V_n = 1.25\sqrt{gd}\log(8.8H/d)$,

ν is the kinematic viscosity, and

d is the size of sediment particles.

The actual discharge of bed load during different seasons of hydrological year is usually smaller than the amount determined from (16). Therefore a correction factor should be introduced in the formula of the deformation rate to obtain correct quantitative results. This correction factor can be estimated by comparing the actual and calculated data for high-water periods.

Assuming that the development of the longitudinal bed profile in the estuary reach and of the mouth bar both start when the depth is still constant along the estuary area, the initial rate of bottom deformations is

$$\varsigma = -\frac{1.5q_{s\_\infty}}{(1-\varepsilon)B_{\_\infty}} U\frac{\partial U}{\partial \tilde{l}}. \tag{17}$$

Method of calculations

Since river depth depends on the flow velocity, which in turn depends on the occurring bottom deformations and varies with both water level and runoff, it was necessary to divide the period of time, during which the mouth bar is developed, into short time intervals such that flow velocity could be assumed constant during each interval. On every next time interval, the flow velocity was recalculated to account for the altered bottom relief, water level, and runoff.

Calculations were performed using the finite differences scheme, which provided stable solutions, as well as the required accuracy.

In the one-dimensional model, the deformation equation (15) was rewritten in this form:

$$\tilde{H}(t+\Delta t,l)=\tilde{H}(t,l)-EU(t,l)\times$$
$$\times\left[U(t,l)\frac{\tilde{H}(t,l)-\tilde{H}(t,l-\Delta l)}{\tilde{H}(t,l)}-\frac{3}{2}\left(U(t,l)-U(t,l-\Delta l)\right)\right], \quad (18)$$

where Δl is the computation step along the longitudinal co-ordinate and Δt is the time step.

The dimensionless quotient E is determined from the initial parameters at the upper boundary of the estuary reach:

$$E=\frac{q_{s_0}\Delta t}{(1-\varepsilon)B_{-\infty}H_{-\infty}\Delta l}=Q\frac{\Delta t}{\Delta l}.$$

A stable solution requires that the parameter E in (18) was sufficiently small. For the actually observed flow velocities and depths, the condition $E\le 1/4$ is sufficient.

Calculations of bottom deformations in the two-dimensional (flow plan) model are more complicated. Variations of jet width due to changing depth and flow velocity requires to calculate a jet depth taking into account the depth of the neighbouring jets.

The relative width of each jet is

$$\tilde{B}_m=1/M\tilde{H}_m\sqrt{U_m}$$

where $\tilde{B}_m=B_m/B_{01}$ is the relative width of an m-th jet,

B_m is the actual width of this jet, and

M is the number of jets in the plan.

The distance between the flow axis and the axis of the m-th jet is $b_m=\frac{\tilde{B}_1}{2}+\sum_{k=2}^{m-1}\tilde{B}_k+\frac{\tilde{B}_m}{2}$.

A new depth of the jet $\tilde{H}'_m(t+\Delta t)$ in the same boundaries is determined from (18). A change in the jet width will be then

$$\Delta\tilde{B}_m(t+\Delta t)=\frac{1/M-\tilde{H}'_m(t+\Delta t)\tilde{V}_m(t)\left[\tilde{B}_m(t)-\Delta\tilde{B}_{m-1}(t+\Delta t)\right]}{\tilde{H}'_{m+1}(t+\Delta t)\tilde{V}_m(t)}.$$

Here we assume that $H'_{\frac{M+1}{2}+1}=1$ outside the jet boundaries and $\Delta\tilde{B}_0=0$. New depths in new boundaries will be

$$\tilde{H}_m(t+\Delta t)=\frac{\tilde{B}_m(t)\tilde{H}'_m(t+\Delta t)+\Delta\tilde{B}_m(t+\Delta t)\tilde{H}'_{m+1}(t+\Delta t)}{\tilde{B}_m(t)+\Delta\tilde{B}_m(t+\Delta t)}.$$

For numerical calculations, the integrals appearing in (7)and (13) (the one-dimensional model) or in (7) and (12) (the two-dimensional model) were replaced by the corresponding sums, and the velocity function U was calculated using the values of hydraulic parameters $\tilde{H}$ and C_k corresponding to the end of the preceding time interval. As there appears an infinite integral in (7), summation started at $\tilde{l}\approx -10..-20$. The velocity and depth upstream from this point were calculated using (8) and (17), respectively.

The results of calculations

Distributions of flow velocities

Numerous experiments were performed to study the velocity field in a flow expansion area. However, most of them either do not conform to our theoretical model or provide insufficient data. Thus, data on the local free-water surface slopes that are crucial for our model are absent from most of these reports. Therefore, we carried out special experiments to establish the effect of bed roughness on the distribution of velocities (averaged over depths) in the flow plan (the experiments used two types of bottoms with the hydraulic coefficients $\lambda_{T_0} = 0.008$ and $\lambda_{T_0} = 0.014$) and to substantiate the values of the turbulence coefficient a accepted in the model.

Theoretical and experimental epures of velocity distributions in the flow plan are shown in Fig. 2. The experimental epures correspond to velocities averaged over depths. The theoretical epures were calculated using (14) with various values of the coefficient a. The best fit is observed at $a = 0.05$ and $C_k'' = 1$. The observed agreement between the calculated and experimental epures indicates that both the accepted phenomenological theory of turbulence and generalisations of the type (10) are valid.

At $a > 0.05$, we observed an increase in the flow expansion angle and significant deviations of the calculated epures from the experiment. Therefore, our attempt to account for the bottom roughness by merely increasing the coefficient a should be considered as a failure.

Bottom relief deformations

We consider the development of a mouth bar in a coastal area with very small bottom slope and assume both the initial depth along the estuary reach and runoff to be constant. These conditions are readily reproduced in laboratory experiments, and sometimes they can be observed in the nature during the formation of a new estuary. The results obtained by solving the one-dimensional model are compared with the experiment in Fig. 3. A good agreement is seen, which indicates validity of the developed model.

An analysis of the calculational results based on the above assumptions most clearly shows how the key factors affect the mouth bar regime. The distribution of flow velocities along the estuary reach and at the mouth bar are shown in Fig. 4. The longitudinal profiles of the estuary reach and mouth bar at various stages of bottom relief formation are shown in Fig. 5 with the key parameters corresponding to the natural conditions.

An analysis of the results based on the one-dimensional model indicates that the maximum free-water surface slope is located exactly at the mouth section in the initial period of the longitudinal bottom profile formation. The greater the surface slope amplitude a_I, the more is the location of maximum flow velocities shifted seawards. In the longitudinal bottom profile, the areas of mouth scouring and bar crest formation are discerned. The initial location of the bar crest depends on both k_T and a_I and is shifted further from the mouth section with decreasing the morphometrical parameter k_T.

Flow velocity in the neighbourhood of the mouth section increases with time, and the location of maximum flow velocity is shifted downstream. The mouth scour is formed at $a_I > 0$. The rate of its formation increases with both k_T and a_I. The intensity of erosion decreases with time. The location of maximum depth migrates seawards with the velocity that is practically independent from time and is mainly determined by the slope amplitude a_I.

The evaluation of mouth bar relief has two stages: 1) the formation of mouth bar by sediment deposition on the initially flat bottom of the coastal area and 2) the seaward migration of the mouth bar thus formed, all its key parameters remaining the same. The bar formation takes the time deter-

mined by k_T and a_I. The final relief is formed more rapidly with increasing k_T and a_I parameters.

The depth at the crest of the formed mouth bar is $\tilde{H}_{cr} = H_{cr}/H_{-\infty} = 0.1..0.12$, which value weakly depends on k_T and a_I. Thus, the depth at the bar crest is slightly decreased with increasing these parameters. The formed mouth bar migrates seawards with a constant velocity, which mainly depends on a_I and increases with increasing this parameter. An insignificant smoothing of the bar crest is also observed.

In the course of mouth bar formation, the rate of bar crest elevation varies and reaches its maximum when the depth at the bar crest is $\tilde{H}_{cr} = 0.4..0.6$. The rate of bar crest elevation increases with increasing both the morphological parameter k_T and slope amplitude a_I. The location of the bar crest with respect to the mouth section is little changed during initial stages of its formation. The value of k_T determines whether the bar will migrate seawards due to sedimentation on its rear slope or approach the mouth section due to preferred sedimentation on the front slope of the bar. The rate of seawards migration of the bar crest increases with time and passes through a maximum prior to becoming constant.

Initially, the rear slope of the mouth bar is very gentle, whereas the frontal slope is steeper. The steepness of both slopes increases with time, that of the rear slope increasing more rapidly. A similar trend was observed in our experiments [6].

The development of a mouth bar in a coastal area sloping towards the sea is shown in Fig. 6. A comparison with Fig. 5 shows that the courses of development and final shapes are different for the bars formed in coastal areas with and without bottom slope.

Calculations for the case when floods of various intensity pass down the river showed that the dynamics of longitudinal bar profile is mainly affected by the level and duration of floods, as well as by sediment discharge. Most intensive restructuring occurs during catastrophical floods when the bar crest is noticeably shifted seawards. Normal floods (not to mention low-water periods) that follow the catastrophic ones practically do not induce any significant bottom deformations neither along the estuary reach nor at the mouth bar.

The results of flow plan calculations are shown in Fig. 7. The initial bottom relief was a flat, nearly horizontal surface. In full agreement with the experiment, maximum sedimentation in the initial period of mouth bar formation occurred in the area of outer jets, where estuary sand bars were formed. As the bottom is elevated with time, its relief starts to affect the flow. The sand bars turn around and migrate along normals to the flow axis, which development is in agreement with laboratory experiments. The bar crest is shifted seawards. The obtained results demonstrate the similarity between physical and numerical modelling in this case.

Conclusions

The results of numerical modelling provide sufficient information on the mouth bar regime, which is necessary for establishing the navigational parameters of a river estuary.

The one-dimensional model describes either a non-branched river delta or the estuary of a single branch. In the latter case, the distributions of river runoff and sedimentation over all delta branches, as well as the free-water surface levels at the heads of the branches during each characteristic season of hydrological year should be available. The described two-dimensional model (flow plan) gives the distributions of flow velocities and bottom deformations both along and across the flow. A number of characteristics of the mouth bar formation were established that depend on the hydrological river factors and the bottom relief of the coastal area.

It should be noted that the development of a mouth bar in coastal areas with sufficiently steep bottoms can not be studied without taking account of the flow breakdown from the bottom, which phenomenon deserves a separate theoretical treatment.

In our opinion, a feasible future extension of this work should be a study of the mouth bar formation and transformation under the influence of wind-induced waves.

References

1. *Deltas Models for Exploration.* Houston: Houston Geological Society, 1975, P. 323.
2. *Rukovodstvo po gidrotekhnicheskim issledovaniyam v pribrezhnoi zone morei i v ust'yakh rek pri gidrologicheskikh izyskaniyakh* (Handbook of Hydraulic Research in Coastal Areas of Seas and River Deltas during Hydrological Survey), Moscow: Gidrometeoizdat, 1972, p. 396.
3. Ivanov V.V., A Hydraulic Calculational Method For Water Regime Characteristics In River Deltas, *Trudy AANII* (Trans. Arctic Antarctic Res. Inst.), 1968, vol. 283, pp. 30-63.
4. Mikhailov V.N., Rogov M.M., and Chistyakov A.A., *Rechnye del'ty* (River Deltas), Leningrad: Gidrometeoizdat, 1986, p. 280.
5. Butakov A.N., Study of Mouth Bar Development and Deformation, *Proc. XIV IAHR Congress,* Paris, 1971, vol. 4, pp. 95-102.
6. Butakov A.N., Mouth Bar Dynamics, *Trudy LIVT* (Trans. Leningrad Inst. Waterways Transport), 1972, vol. 137, pp. 5-18
7. Butakov A.N., *Ruslovye processy v ust'yakh sudokhodnykh rek* (Evolution of River Bed in the Estuaries of Navigable Rivers), Moscow: Transport, 1971, p. 104.
8. Butakov A.N., Mouth Bar Deformations on Northern Rivers, *Peredovoi Opyt Novaya Tekhnika* (Progressive Practice and Novel Technologies), 1979, no. 6, p. 48.
9. Butakov A.N., Velocity Field of a Rapidly Expanding Flow, *Trudy LIVT* (Trans. Leningrad Inst. Waterways Transport), 1970, vol. 126, pp. 43-52.
10. Butakov A.N., Breakdown Flow Plans, *Trudy LIVT* (Trans. Leningrad Inst. Waterways Transport), 1971, vol. 129, pp. 10-15.
11. Butakov A.N., Deformations of Channel Bottom in the Area of Flow Expansion, *Dinamika i termika rek i vodokhranilishch* (Dynamics and Thermal Conditions of Rivers and Reservoirs), Moscow: Stroiizdat, 1973, pp. 149-157.
12. Butakov A.N., On the Formation and Evolution of Accumulative River Beds, *Trudy LIVT* (Leningrad Inst. Waterways Transport Trans.), 1975, vol. 151, pp. 86-94.
13. Butakov A.N., Characteristics of Flow and Bed Formation in River Estuaries, *Rechnaya gidravlika i gidrotekhnika* (River Hydraulics and Hydraulic Engineering), Moscow: Peoples Friendship Univ., 1980, pp. 40-48.
14. Butakov A.N., Mouth Bar Formation upon Active River-Sea Interactions, *Ruslovye protsessy i voprosy gidrotekhniki* (Evolution of River Bed and Hydraulic Engineering Problems), Moscow: Peoples Friendship Univ., 1982, pp. 67-83.
15. Butakov A.N., Theoretical Analysis of Bottom Relief Formation in Expanded River Valleys and Estuaries, *Issledovanie voprosov prikladnoi gidravliki i gidrotekhniki* (Problems of Applied Hydraulics and Hydraulic Engineering), Moscow: Peoples Friendship Univ., 1984, pp. 92-108.
16. Butakov A.N., Numerical Modelling of Mouth Bars, *Proc. V All-Union Congress on Hydrology,* 1989, p. 44.
17. Butakov A.N., The Relation of River Bed Shape to the Hydrological Regime as a Characteristic of River Bed Evolution, *Rezul'taty issledovaniya rechnykh rusel i gidrotekhnicheskikh sooruzhenii* (Studies on River Beds and Hydraulic Structures), Moscow, 1983, pp. 11-27.
18. Levi I.I., *Dvizhenie rechnykh potokov v nizhnikh b'efakh gidrotekhnicheskikh sooruzhenii* (River Flows in the Tail Races of Hydraulic Structures), Moscow: Gosenergoizdat, 1955.
19. Lebedev, I.V., *Rasshirenie potoka v ogranichennom prostranstve* (Flow Expansion in a Limited Space), Moscow: Energy Res. Inst., 1963.

20. Vostorzhel, G.V., Approximate Solution of the Problem of Expanding Water Flow Plan, *Izv. VNIIG* (Bull. All-Union Res. Inst. Hydr.), 1961, vol. 67, pp. 109-120.
21. Mikhalev M.A., *Gidravlicheskii raschet potokov s vodovorotom* (Calculation of Swirling Flow Hydraulics), Leningrad: Energiya, 1971.
22. Sherenkov I.A., *Prikladnye planovye zadachi gidravliki spokoinykh potokov* (Applied Flow Plans of Steady Flows), Moscow: Energiya, 1978.
23. Rakhmanov A.N., Characteristics of Variations in the Length of the Swirling Part of an Expanding Steady Flow, *Izv. VNIIG* (Bull. All-Union Res. Inst. Hydr.), 1965, vol. 78, pp. 83-109.
24. Butakov A.N., Calculation of Flow Jets upon Sudden Flow Expansion, *Meteorologiya Gidrologiya*, 1970, no. 11, pp. 70-76.
25. Makkaveev V.M. and Konovalov I.M., *Gidravlika* (Hydraulics), Leningrad: Rechizdat, 1940.
26. Konovalov I.M., Free Turbulent Fluid Jets, *Trudy LIIVT* (Trans. Leningrad Inst. Waterways Transport Engineering), 1947, vol. 14, pp. 251-253.
27. Konovalov I.M., Turbulent Jets, *Trudy Akademii rechnogo transporta* (Trans. Waterways Transport Academy), 1952, no. 1, pp. 3-11.
28. Reichardt H. *Gesetmässigkeiten der freien Turbulenz.* VDJ Forschungsheft, 1942, S. 414.
29. Hinze J.O., *Turbulence. An Introduction to Its Mechanism and Theory*, N-Y: McGraw Hill, 1959, P.634.
30. Goncharov V.N., *Osnovy dinamiki ruslovykh potokov* (Fundamentals of Bed Flow Dynamics), Leningrad: Gidrometeoizdat, 1954.

Appendix 1. Illustrations

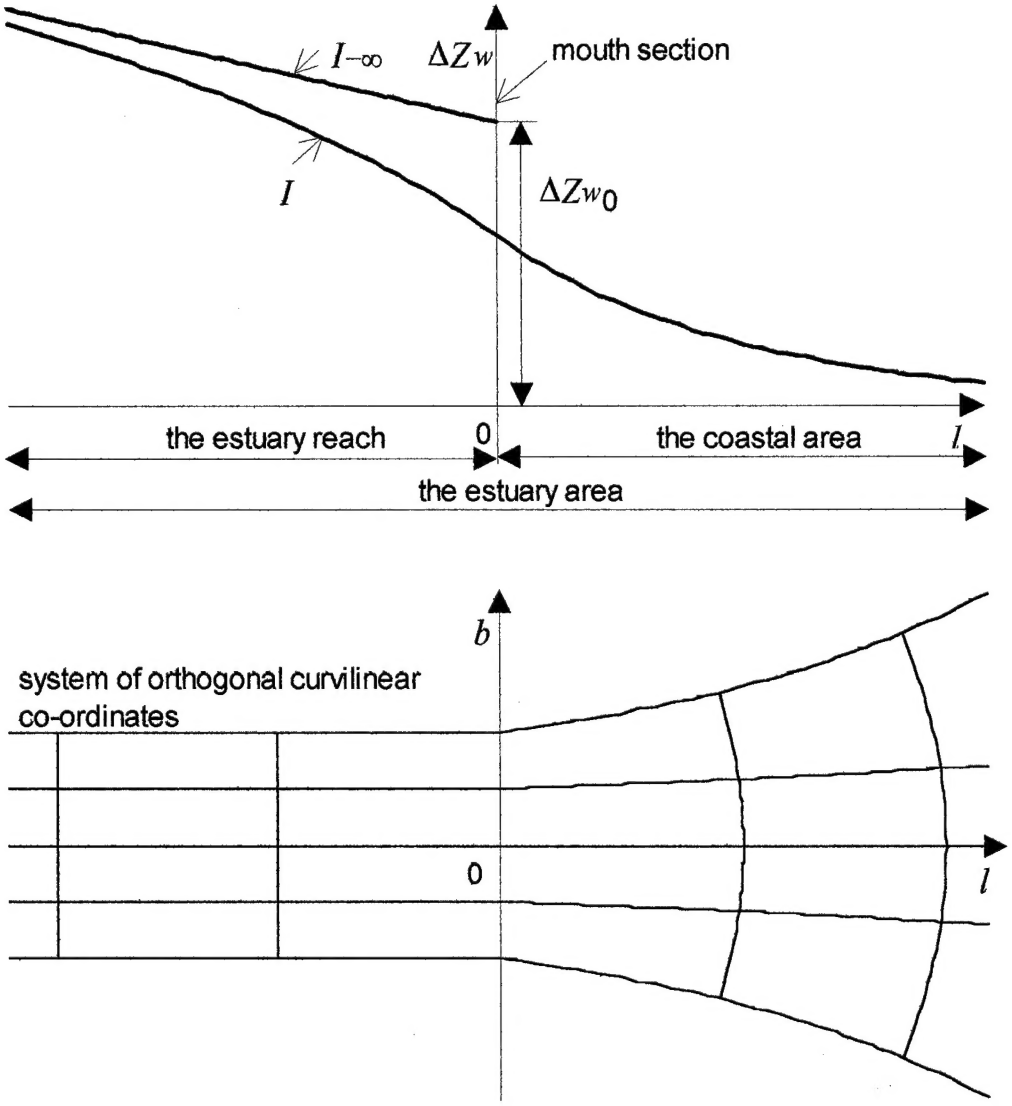

Fig. 1. A system of co-ordinates used in the theoretical model. The longitudinal changes of free-water surface slope.

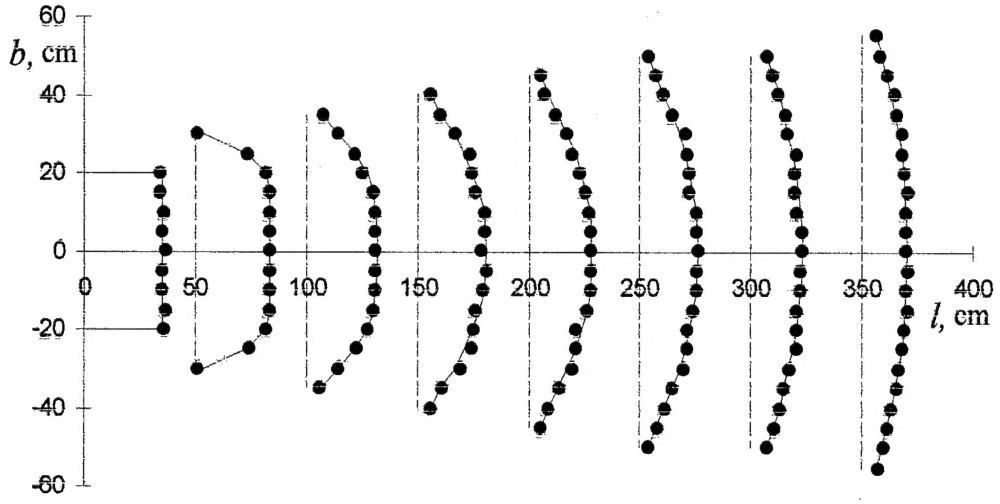

Fig. 2. A comparison of the calculated and experimental velocity distributions along and across the coastal area.

($\lambda_{T_0} = 0.014, a = 0.05$ and $C_k'' = 1$)

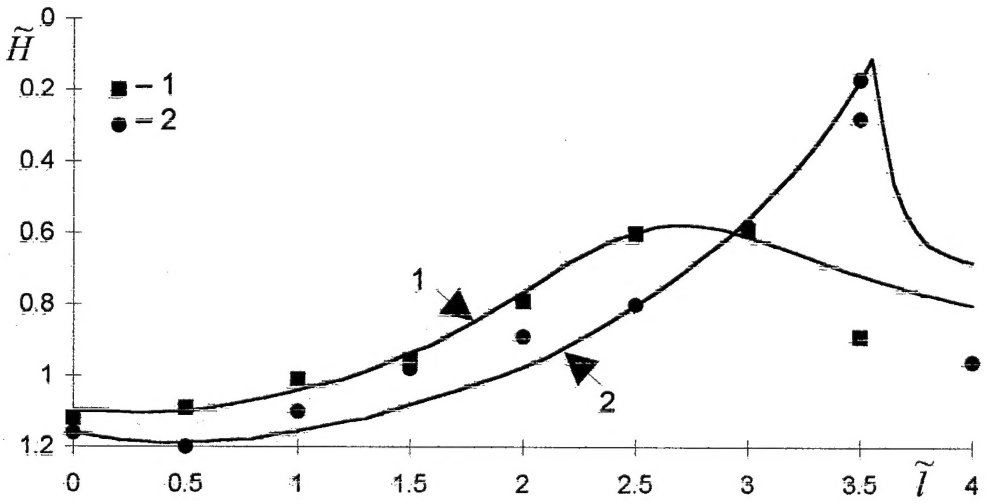

Fig. 3. A comparison of the calculated and experimental bottom deformation.

($k_T = 0.35$, $a_I = 0.25$, 1 – t is 81 hours, 2 – 355 hours)

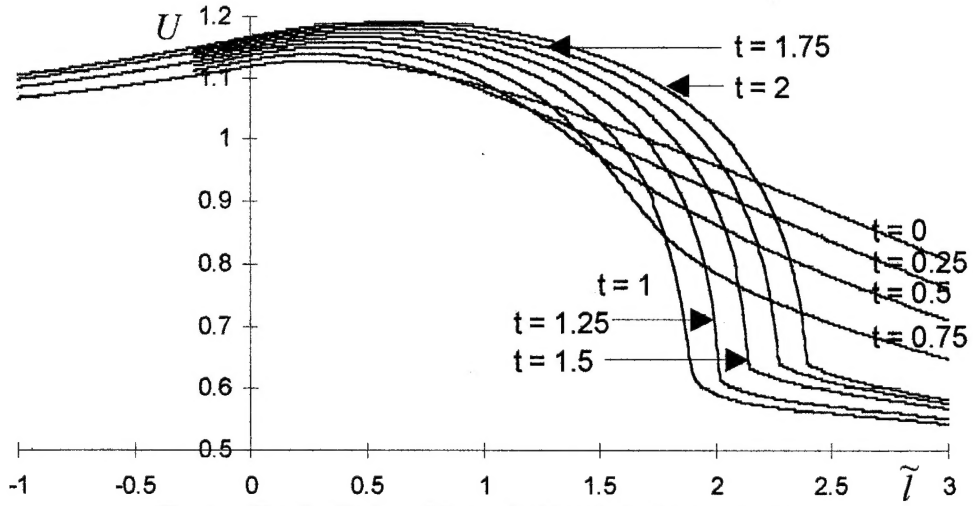

Fig. 4. The distribution of flow velocities along the estuary area.

$(k_T = 0.6,\ a_I = 0.5,\ E = 1.0)$

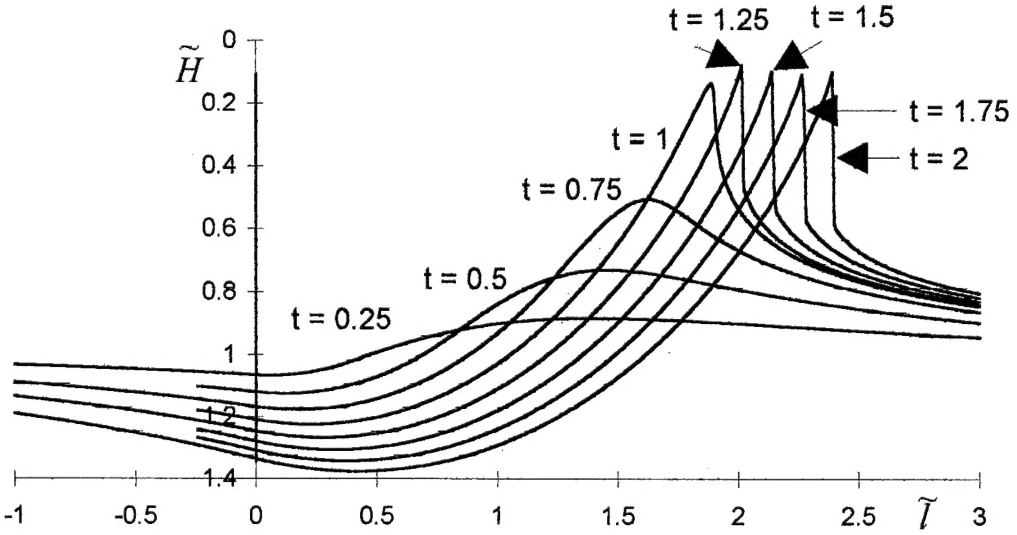

Fig. 5. Bottom deformations along the estuary area.

$(k_T = 0.6,\ a_I = 0.5,\ E = 1.0)$

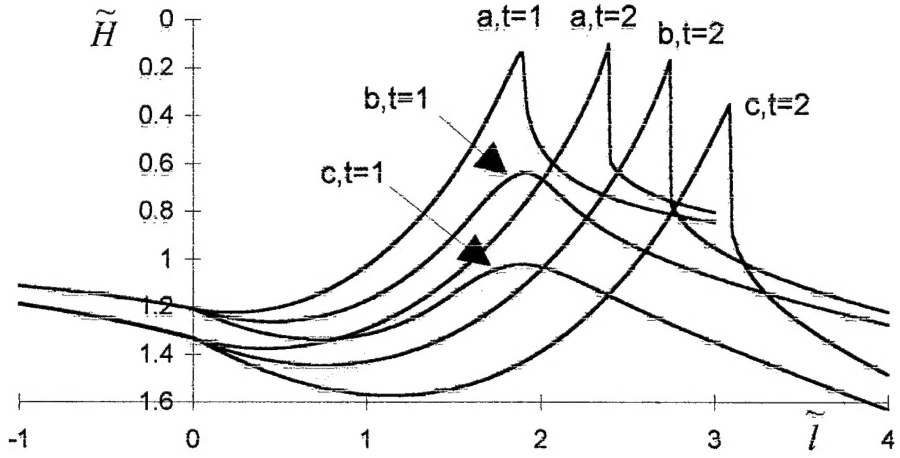

Fig. 6. The effect of initial bottom slope in the coastal area on the evolution of mouth bar relief.
$(k_T = 0.6,\ a_I = 0.5,\ E = 1.0,\ \text{a} - \partial\tilde{H}/\partial\tilde{l} = 0,\ \text{b} - 0.1,\ \text{c} - 0.2)$

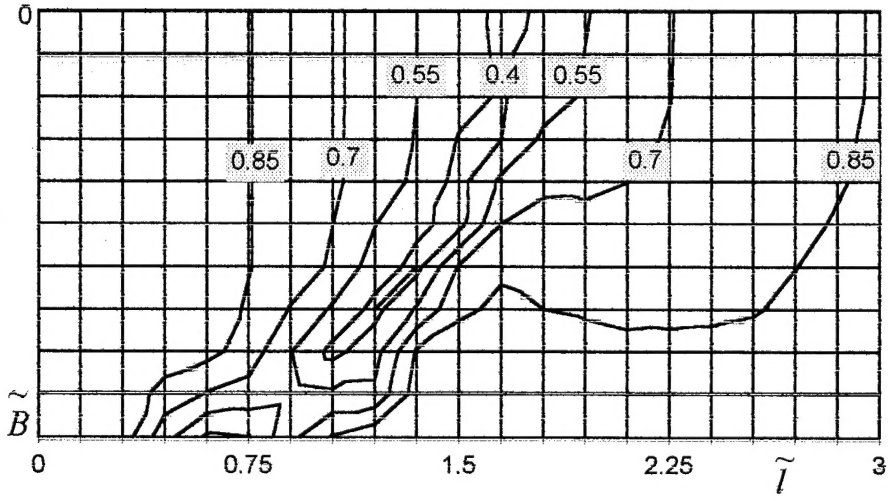

Fig. 7. Bottom deformations along and across the estuary area (the flow plan model).
$(k_T = 0.6,\ a_I = 1.0,\ E = 1.0,\ t = 1.8)$